Improved Results on Finite-Time Synchronization of Shunting Inhibitory Cellular Neural Networks with Time-Varying Delays via Hybrid Impulsive Pinning Control

by

Maikenov Otankhan

M.A., Nazarbayev University (2024)

Submitted to the Department of Mathematics,
School of Science and Humanities,
in partial fulfillment of the requirements for the degree of

Master of Science in Applied Mathematics

at the

Nazarbayev University

April 2024

Author____

Department of Mathematics
April 14, 2024

Certified by____

Ardak Kashkynbayev
Associate Professor
Nazarbayev university
Thesis Supervisor

Accepted by____

Gonzalo Hortelano
Dean, School of Science and Humanities

Improved Results on Finite-Time Synchronization of Shunting Inhibitory Cellular Neural Networks with Time-Varying Delays via Hybrid Impulsive Pinning Control

by

Maikenov Otankhan

Submitted to the Department of Mathematics,
School of Science and Humanities,
on April 14, 2024, in partial fulfillment of the
requirements for the degree of
Master of Science in Applied Mathematics

Abstract

This thesis explores finite-time synchronization in shunting inhibitory cellular neural networks (SICNNs) with time-varying delays. An advanced hybrid controller is introduced to achieve this, serving as a state-feedback and pinning-impulsive controller during impulsive intervals and instants, respectively. Considering the basic Lyapunov function, the paper proposes finite-time synchronization for the SICNNs-based master-slave model structured along with the hybrid controller. This proposition is validated through a series of case studies highlighting the effectiveness of the hybrid controller. Furthermore, this paper compares the settling time of finite-time synchronization using the proposed hybrid controller against the classic state-feedback and pinning-impulsive controller, demonstrating the advantages of the hybrid approach. The effectiveness of the proposed hybrid controller is exemplified through a numerical example, showcasing consensus between MATLAB software simulations and manual computations. The comparison analysis includes assessing the proposed hybrid controller against the classic state-feedback and pinning-impulsive controllers.

Thesis Supervisor: Ardak Kashkynbayev
Title: Associate Professor, Nazarbayev university

Acknowladgements

I am grateful to my research supervisor, Professor Ardak Kashkynbayev, for his advice and support during my thesis work.

I want to express my sincere gratitude to Soundararajan Ganesan for his editing assistance and suggestions to enhance this work.

I thank Professor Md. Hazrat Ali, a second reader, for his useful feedback and ideas on my thesis.

Contents

List of Figures

List of Tables

Chapter 1

Introduction

1.1 Cellular Neural Networks

Nowadays, there is no area where a neural network cannot be applied because of its versatility. Its applications vary from speech recognition and medical diagnosis to defense and aerospace. Neural networks were inspired by the nervous system and their ability to process (1). In addition, most of the recent researches are aimed at better understanding nervous systems' processes, for example, cellular neural networks. Cellular neural networks (CNN) are the one type of neural network used to process information spatially. An illustrative example of CNN is shown in (1-1) (2)(3)(4)(5).

Each cell in this neural network is linked to neighboring cells and conducts local computations, by using a predefined set of parameters. It plays a key role in image processing, because of its features such as segmentation, image filtering, and edge detection. In addition, it has been a widely discussed research topic because of its capability of parallel information processing (2)(3)(4)(5). Since the stability of the neural network is crucial for the applications, the stability of the CNN and other CNN-derived networks has been studied in the last two decades. For example, the global asymptotic stability of CNN (6), complete stability of CNN (7), exponential stability of nonreciprocal CNN (8), exponential stability of continuous-time and discrete-time CNN (9), asymptotic stability of high-order

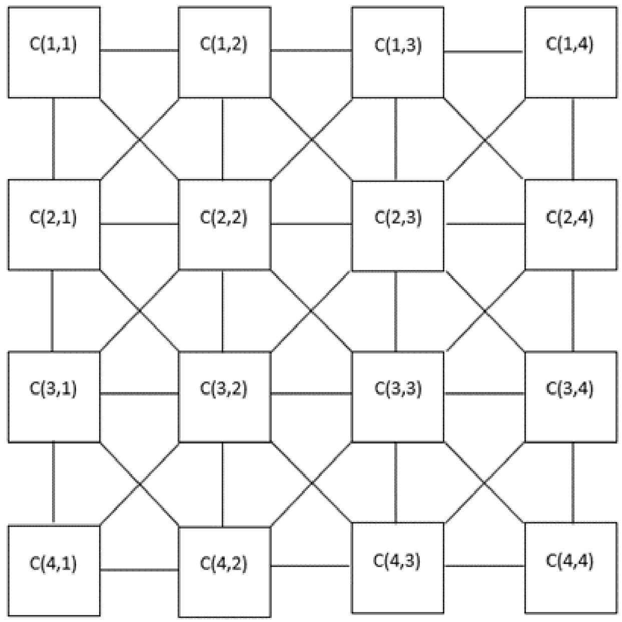

Figure 1-1: Two-dimensional model of cellular neural network.

neutral CNN (10), pseudo almost periodic solutions of quaternion-valued fuzzy CNN (11), and finite-time stability of SICNN (12).

1.2 Shunting Inhibitory Cellular Neural Networks

In 1993 Bouzerdom and Pinter introduced a new class of CNN called shunting inhibitory cellular neural network (SICNN). It is a biologically inspired, CNN-derived type of neural network where there is nonlinear synaptic interaction between the cells. This interaction is called shunting inhibition. The main advantage of this effect is that it increases the robustness of the neural network (13). In addition, it increases the computational efficiency of the network by increasing the conductance of each neuron in the neural network (14). Several articles show its application in the following areas: medical image processing, psychophysics, speech, perception, robotics, adaptive pattern recognition, and vision (15) (16) (17) (18).

Due to its wide range of applications, the dynamic behavior of SICNN has gotten more attention from applied Mathematics researchers. For example, stability of SICNN (15), an anti-periodic solution with time-varying delays (17), almost periodic solution with time-varying delays(19), global exponential stability with delays (20), existence and exponential stability of almost periodic solutions with continuously distributed delays (21), and global stability of almost periodic solution with variable coefficients (22) of SICNN have been studied in the last two decades.

1.3 Impulsive Differential Equation

For the last century, differential equations have been the main tool to model the dynamics of the changing processes. For example, differential equations are used in various areas of biology, physics, statistics, and weather forecasting. However, the dynamics of most real-life and mechanical processes go through abrupt changes, such as natural disasters, harvesting in real-life situations, and collisions in mechanical processes. These changes cause instantaneous increases or decreases in the behavior of the continuous model. These perturbations are called "impulses". The simplest demonstration of the impulses is a Dirac delta function, a function with the value 0 everywhere, except $f(0) = 1$. The demonstrative figure is given in Fig. (1-2).

In modeling dynamical systems, impulses were proposed back in the 1950s, because state dynamics showed sharp changes, that can not be modeled by pure discrete or continuous models. In the 1960s Millman and Myshkis studied differential equations with impulses (23). They were called impulsive differential equations and were first defined by Lakshmikantham et al. in 1989 (24). Since then, impulses and impulsive differential equations have been studied extensively and more deeply. It was found that there exist three factors that are important while researching impulses: impulsive gain, impulsive frequency, and impulsive instant. Here are the importance and a brief explanation of each characteristic based on (25).

The first characteristic is impulsive gain, which is the strength of the impulse, and there exist three categories of impulsive gain: neutral, destabilizing, and stabilizing impulses. Neutral impulses do not affect the model; therefore, they can be called dormant

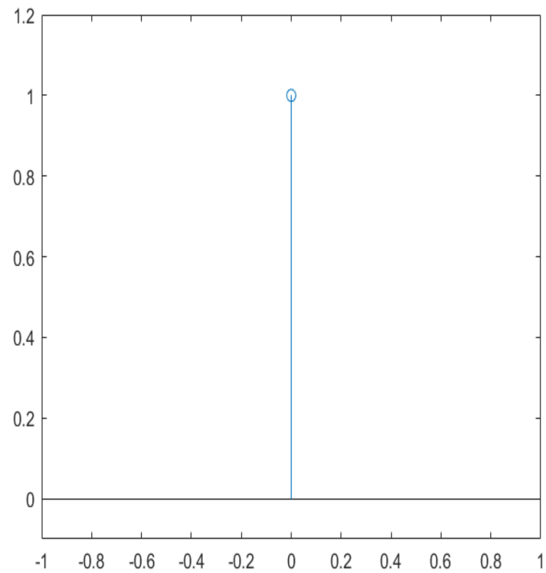

Figure 1-2: Dirac delta function.

impulses. Destabilizing impulses are those that disrupt the stability of the model and can result in unexpected and undesired behavior. Meanwhile, stabilizing impulses enhance the stability of the model. To distinguish impulsive gain one from another absolute value notation is used: if the absolute value impulse gain, let us take as μ, is equal to 1, then it is a neutral impulse; if $|\mu| > 1$, then it is called a destabilizing impulse; if $|\mu| < 1$, then it is called a stabilizing impulse. In (26) authors found necessary and sufficient conditions for stability for each of these three categories.

The second characteristic is impulsive frequency, a key indicator for defining an impulse sequence, which denotes how often the impulses will be applied. Because one is interested in attaining certain results by including impulses in the model. In this case, if the frequency is exceedingly low, the impulses' influence on the model is insignificant, and the intended outcome cannot be accomplished. However, if the frequency is set too high, the model will be computationally difficult, even if the desired outcome is achieved. Therefore, the number of impulses required to accomplish a given result has been an important subject in the field of impulse systems. Lu et al, in (27) presented a novel way to bound the impulsive frequency, which is called an average impulsive interval. It bounds the number of impulses from above and below, and it gives flexibility to change boundaries and allows to change the boundaries simultaneously. By using an average impulsive interval, Lu et al. developed a unified synchronization criterion for impulsive systems that is independent of the type of impulse gain.

Definition 1 *(28)An impulse sequence* $\{t_k, k \in \mathbb{N}_+\}$ *is said to have average impulsive interval* T_a *if there exist a positive integer* N_0 *and positive constant* T_a *such that*

$$\frac{t - t_o}{T_a} - N_0 \leq N(t_0, t) \leq \frac{t - t_o}{T_a} + N_0,$$

where $N(t_0, t)$ *is the number of impulsive instants of the impulse sequence* $\{t_k, k \in N^+\}$ *in* (t_0, t)*.*

The third characteristic is impulse instant, which decides how the impulses will be applied. There are two types of impulse instant sequence: when the sequence is fixed and when the sequence is calculated. The calculated time is determined by whether the system intersects a particular surface. However, this method is usually used for the stabilization of unstable systems. Because our major purpose for adding impulses in the thesis work varies from this, here we will apply a fixed impulse instant sequence.

The system where the impulse is involved is called an impulsive system and it has acquired many research interests because of its variety of applications, including in biology, communication networks, control technology, and engineering sciences. The stability of the impulsive system plays a key role in applications, and as a result, it has been researched in many articles and books (25) (24)(23)(29)(30). Overall, articles about the stability of impulsive systems can be divided into two main topics: impulsive perturbations and impulsive control. The first topic evaluates impulsive systems with destabilizing effects and researches their stability. Meanwhile, articles on the second topic, impulsive control, contemplate impulses with stabilizing effects (29).

1.4 Basics of Impulsive Differential Equation

Impulsive differential equations play a key role in modeling sudden changes in continuous behavior. Unlike ordinary differential equations, which model continuous processes, impulsive differential equations can include instantaneous jumps in the model. As a result, impulsive differential equations have gained a lot of amounts of research attention because of their variety of applications in fields, such as physics, population dynamics, ecology, biological systems, and biotechnology (31)(32). For example, in population dynamics impulsive differential equations can explain sudden death caused by natural disasters.

An example of an impulsive differential equation is shown below

$$\begin{aligned} x'(t) &= f(t,x), && t \neq t_k, \\ \Delta x|_{t=t_k} &= J_k(x(t_k^-)), && t = t_k, k \in \mathbb{Z}^+, \end{aligned} \tag{1.1}$$

where $f(\cdot,\cdot)$ is a given function, $\Delta x = x(t_k^+) - x(t_k^-)$, $x(t_k^+) = \lim_{h\to 0} y(t_k + h)$ and $x(t_k^-) = \lim_{h\to 0} y(t_k - h)$ are right and left limits of $x(t_k)$ at $t = t_k$, respectively, t_k is a impulse instant sequence, $k = 1, 2, ...$ The impulsive differential equations consist of ordinary or delay differential equations, which work at all times except impulse times, and the difference equation, which works at impulse times. This impulse time is usually referred to as an impulsive sequence and consists of discrete time sequences in increasing order.

1.4.1 Existence and Uniqueness of a Solution

Let the functions $f(\cdot,\cdot)$ and $J(\cdot)$ from (1.1) be $f : I \times G \to \mathbb{R}^n$ and $J : \mathcal{A} \times G \to \mathbb{R}^n$, where $I \subset \mathcal{R}$ is an open interval, $G \subset \mathcal{R}^n$, and $\mathcal{A}$ is a set of indexes k. Then the domain of the impulsive differential equation (1.1) is the set $\Omega = I \times \mathcal{A} \times G$. Fix $(t_0, x_0) \in I \times G$, and let

$$I_0 = [t_0 - h, t_0 + h], G_0 = \{x \in \mathcal{R}^n : ||x - x_0|| < H\},$$

with some fixed positive numbers H and h. Assume that the numbers are small such that $I_0 \times G_0 \in I \times G$. Let $p_+ = N([t_0, t_0 + h]), p_- = N([t_0 - h, t_0]), \mathcal{A}_0 = \{k \in \mathcal{A} : t_k \in I_0\}$, and $k \in \mathcal{A}_0$, where $N([\cdot, \cdot])$ is as in (1).

(C1) $||f(t,x) - f(t,y)|| \leq l||x - y||$, $||J_k(x) - J_k(y)|| \leq l_1||x - y||$, for arbitrary $x, y \in G$, uniformly in all $(t,k) \in I \times \mathcal{A}$.

(C2) $sup_{J\times G}||f(t,x)|| + sup_{\mathcal{A}\times G}||J_k(x)|| = M < \infty$.

Theorem 1 *[Existence and uniqueness] (32) Let conditions (C1),(C2), and the inequalities*

$$M(h + max(p_+, p_-)) < H,$$

$$lh + l_1 max(P_+, p_-) < 1,$$

be valid. Then the initial value problem (1.1) *and* $x(t_0) = x_0$ *admit a unique solution on* I_0.

1.4.2 Comparison Theorem for the Impulsive Differential Equation

Similar to the ODE, we use a comparison system to solve an impulsive differential equation. The main contribution of this comparison system is that it simplifies the more complex system and approximates its solution.

Lemma 1 *[Comparison system] (28) Let* $0 \leq \gamma(t) \leq \overline{\gamma}$. $F(t, u_1, u_2) : R^+ \times R \times R \to R$ *and* $I_k(u) : R \to R$ *be nondecreasing in* u. *Suppose that*

$$\begin{cases} D^+u(t) \leq F\Big(t, u(t), u\big(t - \gamma(t)\big)\Big), & t \neq t_k, \\ u(t_k) \leq I_k\big(u(t_k^-)\big), & k \in N, \end{cases} \tag{1.2}$$

$$\begin{cases} D^+v(t) > F\Big(t, v(t), v\big(t - \gamma(t)\big)\Big), & t \neq t_k, \\ v(t_k) \geq I_k\big(v(t_k^-)\big), & k \in N, \end{cases} \tag{1.3}$$

then $u(t) \leq v(t)$ *for* $-\overline{\gamma} \leq t \leq 0$ *implies that* $u(t) \leq v(t)$ *for* $t > 0$, *where* $D^+u(t) = \overline{lim}_{h\to 0^+} \frac{u(t+h)-u(t)}{h}$.

1.5 Delay Differential Equation

In modeling the dynamics of changing processes, delays, and dependence on history, are one of the essential effects, since delays are an important phenomenon in many fields, such as biological networks, finite chemical reaction times, and the stock market (33) (34). In addition, since time is required to process the information and to react to it, time delays are inevitable when feedback control is considered (35). Delay differential equations come in the following form

$$x'(t) = f(t, x(t + \tau)), \tag{1.4}$$

where $f(\cdot, \cdot)$ is a given function, and τ is a delay term. Here we generalize delay by term τ, because, there are several types of delay: a constant delay, which can be expressed as $\tau = -\beta$, proportional delay, that is $\tau = -\beta t$, and time-varying delay, that is $\tau = -\gamma(t)$. Here β and $\gamma(t)$ are a positive constant and a function, respectively.

1.5.1 Existence and Uniqueness of a Solution.

Let r be a given positive real number and $C([a, b], \mathcal{R}^n)$ be a Banach space of continuous functions mapping $[a, b]$ into the $\mathcal{R}^n$. If $\sigma \in \mathcal{R}$, $A \geq 0$, and $x \in C([\sigma - r, \sigma + A], \mathcal{R}^n)$, then for every $t \in [\sigma, \sigma + A]$ assume that $x(t + \tau) \in C$, where $-r \leq \tau \leq 0$. Let $D \subset \mathcal{R}^n \times C$ and the function f from (1.4) be $f : D \to \mathcal{R}^n$. We seek a solution $x(t)$ of (1.4) satisfying

$$x(t) = \phi, \sigma - r \leq t \leq \sigma, \tag{1.5}$$

and satisfying (1.4) on $\sigma \leq t \leq \sigma + A$ for some $\phi \in C$.

Theorem 2 *[Existence and uniqueness] (36) Suppose that Ω is an open set in $\mathcal{R} \times \mathcal{C}$, $f : \Omega \to \mathcal{R}^n$ is continuous, and $f(t, \phi)$ is Lipschitizian in ϕ in each compact set in Ω. If $(\sigma, \phi) \in \Omega$, then there is a unique solution of Equation* (1.4) *through (σ, ϕ).*

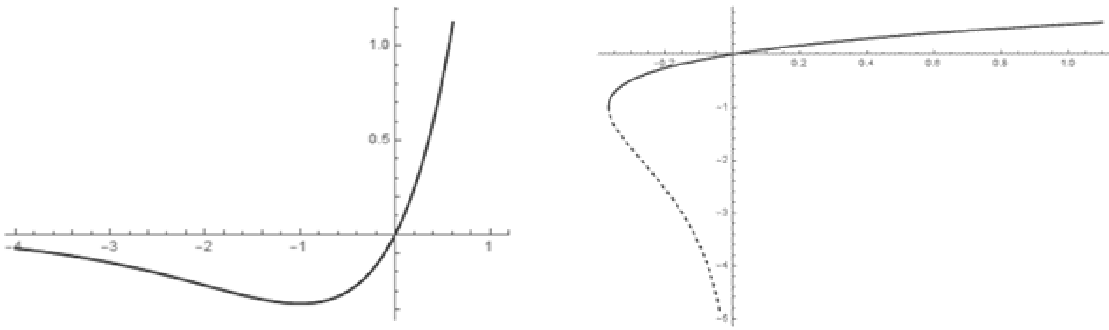

(a) (b)

Figure 1-3: (a) The graph of $f(x) = xe^x$. (b) The Lambert W function and its real-valued branches: the continuous plot is $W_0(x)$, and the dashed plot is $W_{-1}(x)$.

1.6 Special Functions

In this thesis work a special function, named Lambert W function, is used. By using (37) an overview of Lambert W function is given below.

Definition 2 *(Lambert W function) Let the $f(x) = xe^x$. Then the Lambert W function is defined as the inverse of $f(x)$ and noted as $W(x)$.*

This function is used to solve equations that involve exponential terms and delay differential equations (DDE). In addition, it can be applied to solve problems in physics, biology, probability, and combinatorics. For example, in biology Lambert W function is used to deal with cell growth. In general, the cells' population behavior is modeled by ordinary differential equations (ODE). However, it was observed that some cells go through step-like growth at the beginning, and as a result, ODE is not applicable. Therefore, in this situation, DDE models cell growth more accurately than ODE. To solve this kind of DDE one needs to apply the Lambert W function.

If we try to solve the equation $xe^x = a$, we can find that there exist infinitely many solutions to this equation. Among these solutions, there will be at most two real solutions. Therefore, one can notice that this function is not invertible since it is not one-to-one (Fig. 1-3). To make it one-to-one we divide the domain into pieces, and then in it piece it will be an invertible function. Each invertible piece is called a branch. Lambert W function has two branches that take only real values, and in Fig. 1-3 in the second graph these branches can be seen, they are called W_0 and W_{-1} branches of the Lambert W function.

Definition 3 *(37) (Branch-Cut of Lambert W function) A branch of the Lambert W function refers to a specific portion of its multi-valued nature. The Lambert W function, denoted as $W(x)$, has several branches, each corresponding to different ranges of input values. The most common branches are 0 and -1 branches, denoted as $W_0(x)$ and $W_{-1}(x)$, respectively, where*

$$W_0 : \Big[-\frac{1}{e}, +\infty\Big) \to \Big[-1, +\infty\Big),$$
$$W_{-1} : \Big(-\frac{1}{e}, 0\Big) \to \Big(-\infty, -1\Big).$$

One of the features of the Lambert W function is that this function is transcendental. It means that the values of this function cannot be found algebraically. To find exact values some other software is needed, such as MATLAB, or a special calculator, such as Wolfram Alpha, can be used.

1.6.1 Example

Here is an example of how the Lambert W function can be used to solve equations.

$$3^x = 7x.$$

Since the Lambert W function is the inverse of the equation with exponential expression, we need to rewrite it with base e.

$$e^{xln3} = 7x.$$

Rewrite this expression as $ae^a = b$, where a is the expression in terms of x, and b is a specific number.

$$\frac{1}{7} = xe^{-x\ln 3}.$$
$$-\frac{\ln 3}{7} = (-x\ln 3)e^{(-x\ln 3)}.$$

Since $-\frac{1}{e} < -\frac{\ln 3}{7} < 0$, the above equation have two real solutions are $x_1 = -\frac{W_0(-\frac{\ln 3}{7})}{ln3} \approx 2.66266637482$ and $x_2 = -\frac{W_{-1}(-\frac{\ln 3}{7})}{ln3} \approx 0.17270423966$. The values of $W_0(-\frac{\ln 3}{7})$ and $W_{-1}(-\frac{\ln 3}{7})$ were found by using special calculator for Lambert W function.

1.7 Control Theory

Manipulating the dynamics of the model to get a desired output is called control theory. The following differential equation serves as a starting example of control theory

$$\dot{x(t)} = f(x(t), u),\ x(0) = x_0 \in \mathcal{R}^n, \tag{1.6}$$

where x is a state variable, u is a control such that $u \in U \subset \mathcal{R}^m$, and U is called the set of control parameters.

A brief overview of (38) and (39) is presented to explain the concept of control. Depending on the relation between the system and the control, controls are classified into two types: open-loop and closed-loop controllers (see Fig. (1-4)). In open-loop controllers, only the input causes the control to be applied and u from (1.6) can be an arbitrary function $u : [0; +\infty) \to U$. In closed-loop controllers, the so-called feedback phenomenon occurs. In this situation, the controller sets up the input by rerunning the output as an input, and in the case of (1.6) u is defined as $u = u(x(t))$. Closed-loop controllers are more adaptive and more stable in the presence of disturbances. As a result, these controllers are said to have a stabilizing effect. However, controllers designed in a closed-loop way need more computational time than open-loop controllers. Despite this, a closed-loop controller is preferable when precision and stability are required. In neural networks, controllers are

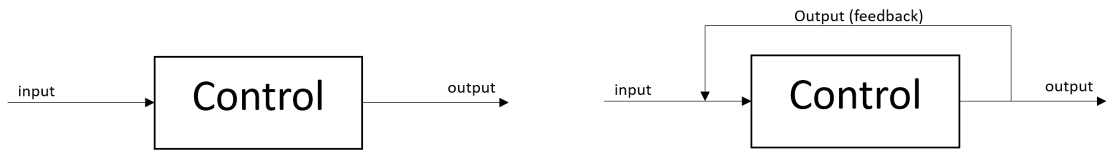

(a) (b)

Figure 1-4: Types of controllers: a) open-loop controller, b) closed-loop controller.

usually used in problems of stability or synchronization

Definition 4 *(38) The system* (1.6) *is said to be stable if there exist* $x_0 \in \mathcal{R}^n$ *and* $u_0 \in U$ *such that* $f(x_0, u_0) = 0$.

1.8 Synchronization

From the existing literature, we can see that the synchronization problem is one of the most researched problems in the field of neural networks. Consider the following system of differential equations

$$\begin{aligned} \dot{x} &= f(t, x(t)), \\ \dot{y} &= f(t, y(t), u(t)), \end{aligned} \tag{1.7}$$

where x, y, and u are from $\mathcal{R}^n$. The synchronization problem consists of two states: the state x with given dynamics, the state y with controllable dynamics, and a control u. By applying u, the control, the dynamics of y is forced to merge with the dynamics of x, or in other words we decrease the error between these two states. An illustrative example is shown in Fig. 1-5. One of the applications of neural networks is image encryption, where we deal with distributed and/or parallel computing. In this example, without a proper synchronized system, the outcome of the encrypted image will be anarchic.

The synchronization can be categorized into three types:

- complete synchronization: all states are synchronized into one trajectory,

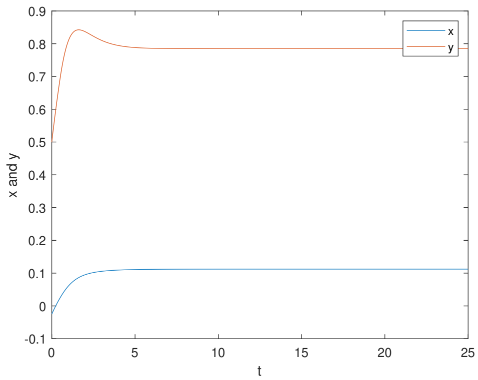

(a)

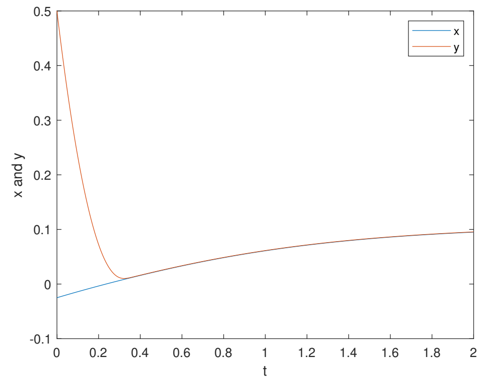

(b)

Figure 1-5: a) The system is not synchronized since the error between two states does not tend to be zero. b) The system is synchronized because the error becomes zero after some amount of time.

- generalized synchronization: the output of the one state and the output of the other state become identical,
- phase synchronization: phase dynamics of two oscillatory systems become synchronized, meanwhile, frequencies and amplitudes can be not synchronized.

In this thesis, we are interested in generalized synchronization. It is often referred to as a master-slave system, where the master system is a given state dynamics and the slave system is a controlled dynamics.

There are two types of synchronization, depending on the time required to synchronize: asymptotic synchronization and finite-time synchronization. Define the error state $e(t)$, where $e(t) = y(t) - x(t)$ and $y(t), x(t)$ as in (1.7).

Definition 5 *The system* (1.7) *achieves asymptotic synchronization if* $\lim\limits_{t\to+\infty}\sum_{i=1}^{n}||e_i(t)|| = 0$ *and* $\sum_{i=1}^{n}||e_i(t)|| > 0$ *for all* $t < +\infty$.

Definition 6 *The master-slave system* (1.7) *is said to be finite-timely synchronized if there exists a constant* T *such that* $\lim\limits_{t\to T}\sum_{i=1}^{n}||e_i(t)|| = 0$ *and* $\sum_{i=1}^{n}||e_i(t)|| = 0$ *for* $t \geq T$*, where* T *is a settling time, which depends on the initial value of the system,* In one of the applications of synchronization, in secure communication, the time needed to recover or send the encoded message depends on the time of the synchronization process. Therefore finite-time synchronization is crucial in secure communication (40). In addition, it is observed that systems synchronized in finite time perform better even if uncertainties and disturbances exist (41). Because of this, finite-time synchronization is becoming one of the most interesting topics in synchronization problems (42)(43).

1.8.1 Examples

Example 1. Let us consider a two-dimensional coupled differential equations

$$\begin{aligned} \tfrac{dx_1}{dt} &= x_2 - x_1 \\ \tfrac{dx_2}{dt} &= x_1 - x_2, \end{aligned} \tag{1.8}$$

where x_1 and x_2 are state variables. Even if the initial conditions of these two states are different, the rate of change of each state will push them toward each other. Eventually, the values of the states will converge to one value, resulting in asymptotic synchronization.

Example 2. Let us consider the following initial value problem

$$\begin{aligned} \tfrac{de}{dt} &= e + u, \\ e(0) &= 5, \end{aligned} \tag{1.9}$$

where e is an error state, and u is a control. Define the control as $u = -e - 2$. Then substitute the control into the (1.9) and integrate with respect to t.

$$\begin{aligned} \frac{de}{dt} &= e + u = e + (-e - 2) = -2, \\ \int \frac{de}{dt} dt &= \int (-2) dt, \\ e(t) &= -2t + C. \end{aligned}$$

By applying the initial value we obtain that $e(t) = -2t + 5$. Now we need to find the settling time, T, which is $T = 2.5$ sec. After 2.5 seconds the error will be zero, resulting in finite-time synchronization.

1.9 Lyapunov Function

Let that in (1.1) $f : \mathbb{R} \times \mathbb{R}^n \to R$ is continuous and $f(t, 0) = 0$.

Definition 7 *The function $W : \mathbb{R}^n \to R$ is said to be positive definite on $\mathbb{R}$ if $W(x) > 0$ for all nonzero $x \in \mathbb{R}^n$ and $W(0) = 0$.*
$W(x)$ is said to be positive semi-definite if $W(x) \geq 0$ for all $x \in \mathbb{R}^n$.
$W(x)$ is said to be negative semi-definite if $W(x) \leq$ for all $x \in \mathbb{R}^n$.

Theorem 3 *(25) Assume that a positive definite function $V(t, x)$ defined on $\mathbb{R}_+ \times \mathbb{R}^n$ satisfy*

$$\dot{V}(t, x) \leq 0, t \neq t_k,$$

and

$$V(t_k^+, x + J_k(x(t_l^-)) \leq V(t_k, x),$$

Then the trivial solution to the system (1.1) is stable.

1.9.1 Example

Let us look at the following example.

$$\begin{aligned} \dot{x}(t) &= -x(t), & t \neq t_k, \\ x(t_k) &= 0.5x(t_k^-), & t = t_k, \end{aligned} \tag{1.10}$$

where $t_k \in \mathbb{Z}^+$. *Solution.* Let us take the Lyapunov function $V(t, x) = \frac{1}{2}x^2$. By taking the time derivative for $t \neq t_k$ one can derive the following equation

$$\dot{V}(t, x) = x\dot{x} = -x^2.$$

For $t = t_k$ by applying impulses, the following equation is obtained

$$V(t_k, x(t_k)) = \frac{1}{2}\big[x(t_k)\big]^2 = \frac{1}{2}\big[\frac{1}{2}x(t_k^-)\big]^2 = \frac{1}{4}\frac{1}{8}\big[x(t_k^-)\big]^2 = \frac{1}{4}V(t_k^-, x(t_k^-)).$$

Then by Theorem 3, the trivial solution of the (1.10) is stable.

Chapter 2

Hybrid Impulsive Pinning Control

There are several types of controllers, and the common two types of controllers are as follows: the first is continuous time controllers, such as feedback control, adaptive feedback control, and state feedback control; the second is discrete-time controllers, such as impulsive control, and intermittent control (33). The main difference between continuous and discrete time controllers is in the modeling. The continuous controller is modeled by a differential equation, and discrete controllers are modeled by a difference equation. Additionally, continuous controllers are easy to monitor and easy to adapt. Since discrete controllers are applied only at discrete-time sequences, discrete controllers are cost-effective and researches show that they are less sensitive to disturbances (44). However, unlike continuous controllers, discrete controllers are applied at a predefined set of points, such as the impulsive sequence in impulsive control or impulsive differential equations. Therefore, its adaptability is limited compared to continuous controllers.

Recently, one has been interested in upgrading control by decreasing control costs or by decreasing settling time for synchronization (34) (45) (46). Therefore, a new type of control, namely hybrid control, was introduced. Hybrid controls are obtained by combining two or more controls, which means that the components of hybrid control are inconsistent and can be changed if necessary. In this thesis, we are proposing a novel hybrid control, which consists of feedback, impulsive, and pinning controls.

2.1 Feedback Control

The feedback control is a continuous closed-loop control. This is one of the first techniques which was introduced in the control theory (47). In addition, feedback control is common in literature because it is easier to design (48) (49) (50). The feedback control operates as follows: after computing the model output, it modifies the input data by adding parameters or substituting a specific function. There are several types of feedback control, such as state feedback, and adaptive feedback. In the system with the state-feedback controller, the parameters are fixed (51). However, in the case of the adaptive feedback controller, the system can easily change parameters using its response to achieve the desired output (52).

2.1.1 Example

Here is a simple example of stabilizing the unstable differential equation with feedback control. Let us consider the following unstable system

$$\frac{dx}{dt} = ax - u, \tag{2.1}$$

where x is a state variable, a is a constant, and u is a feedback control that will be designed later. Let us consider several cases of designing the feedback control:

- **u=0:** The rate of change of the state is directly proportional to the current value of the state. In this case, if $a > 0$ the model will be unstable.
- $\boldsymbol{u = bx}$ **and** $\boldsymbol{b < a}$**:** $ax - bx$ is positive, therefore the rate of change is positive, and the model is unstable.
- $\boldsymbol{u = bx}$ **and** $\boldsymbol{b \geq a}$**:** $ax - bx$ is zero or negative, therefore the system is already stable, or will gradually be stabilized.

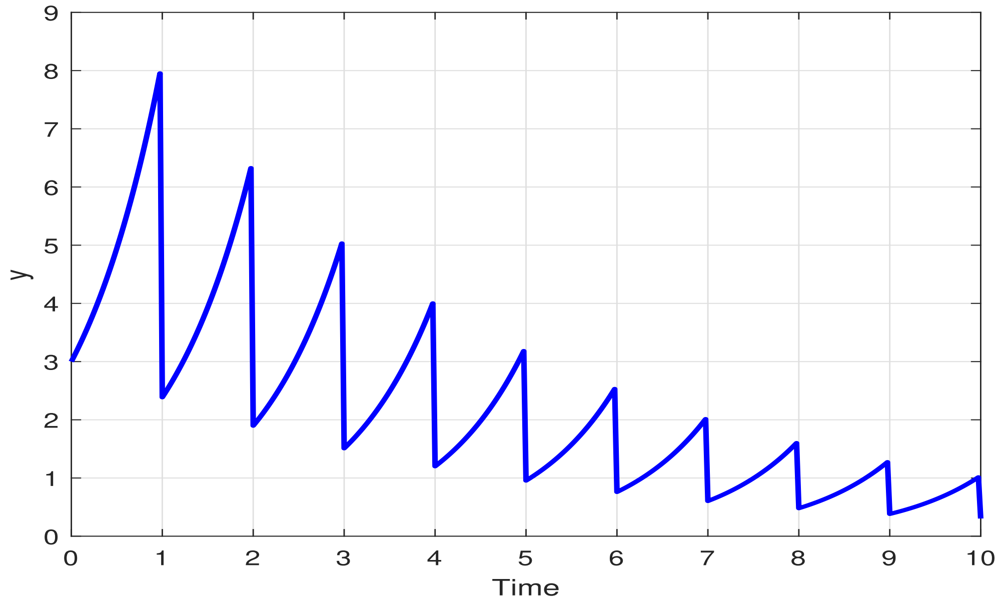

Figure 2-1: The graph of e satisfying the system (2.2)

2.2 Impulsive Control

The impulsive control is discrete open-loop control, and Yang's academic publication from 2001 has the earliest reference to this control approach (53). Impulsive control adds impulses to the system at discrete points in time. Following (25), we summarize the benefits of impulsive control as follows:

- The impulsive controller has a basic form and an easy-to-implement control mechanism.
- Systems with impulsive control are highly robust to the disturbances.
- In comparison to other controls, impulsive control increases reaction time and decreases information redundancy.
- Impulsive control systems are more secure since they limit information transmission.

- In many cases, impulsive control can provide an effective approach to overcome the issues that some dynamical systems cannot handle with continuous-time control.

Because of the aforementioned advantages, impulsive control became a widely researched topic. Therefore, several papers studied different types of stability with impulsive control: exponential stability (54), input-to-state stability (55), stability of two measures (56), finite-time stability (57), bifurcation of the system (58), and chaos phenomena (59).

2.2.1 Example

Here is an example of asymptotic synchronization via impulsive control. Consider a simple error system

$$\begin{aligned} &\tfrac{de}{dt} = 0.5e, \qquad t \neq t_k, \\ &\Delta e = -0.7e, \quad t = t_k, \\ &e(0) = 3, \end{aligned} \tag{2.2}$$

where e is an error state and t_k is an impulsive sequence which is a set of positive integers. The dynamics of the error states in Fig. (2-1) are reaching stable solution 0. This means that the system achieves asymptotic synchronization via impulsive control.

2.3 Pinning Control

Proposed in 1997 by Grigoriev et al. pinning control is another method to achieve synchronization (60). Pinning control is discrete time control, however, it cannot be categorized into open-loop or closed-loop control. Because depending on the situation it can be both. The main idea of this control is to reduce the number of controls applied to the system by pinning a part of the model. At the pinned part of the system, controls will be applied by a predefined strategy. A vast amount of literature has been published proposing new strategies to synchronize with pinning control (61)(62)(63)(64). Because pinning control is about selecting a specific portion of the system, it has no effect on the system's behavior if no other controls are used. Therefore, most of the recent articles about synchronization consider a combination of pinning control with other controls. For example, pinning and impulsive control (65) (28), pinning and feedback control (62) (33), pinning and intermittent control (66).

2.4 Hybrid Impulsive Pinning Control

In this thesis work these three controls are involved to improve previous results. By combining three types of controls, and using the advantages of each, we are proposing a novel hybrid pinning impulsive control to achieve finite time synchronization in SICNN. Pinning control is an efficient method for dealing with high-dimensional models. Impulsive control is an energy-saving control since it admits discontinuities and reduces errors quickly (28) (67). Finally, because pinning and impulsive controls are ineffective for attaining finite-time synchronization, adaptive feedback plays a key role in achieving this problem.

2.5 Novelty of the thesis

The main contributions of this thesis are summarized as follows:

(1) An advanced hybrid impulsive pinning control is introduced to achieve finite-time synchronization in SICNNs with time-varying delays.

(2) Comparison analysis of the hybrid impulsive pinning control, impulsive feedback, and classical feedback control is done. As a result general criterion is given to show the superiority of hybrid impulsive pinning control compared to other controls.

Chapter 3

Synchronization Analysis

In this section, we define the SICNN model equation. In addition, the necessary definitions and lemmas that will be useful for the rest of the research are given.

The state representation of the dynamics of time-varying delayed SICNNs with mn cells can be expressed as follows:

$$\frac{dx_{ij}(t)}{dt} = -\alpha_{ij}(t)x_{ij}(t) - \sum_{C_{hl}\in N_r(i,j)} C_{ij}^{hl}(t)f_{ij}\big(x_{hl}(t-\gamma_{hl}(t))\big)x_{ij}(t) + I_{ij}(t), \tag{3.1}$$

where $x_{ij}(t)$ denotes the voltage/activity of the cell $C_{ij}(t)$; the positive scaalar function $\alpha_{ij}(t)$ denotes the passive decay rate of the cell activity; the time-dependent variable $C_{ij}^{hl}(t) > 0$ denotes the connection or coupling strength; $\gamma_{hl}(t)$ denotes the transmission delay; $f_{ij}(\cdot)$ is the activation function; $I_{ij}(t)$ is the external input to the cell $x_{ij}(t)$. $N_r(i,j)$ denotes the r neighborhood of the cell, which is defined as follows:

$$N_r(i,j) = \{C_{hl}(x_{ij}(t)) : \max\{|h-i|, |l-j|\} \le r,\ 1 \le h \le m,\ 1 \le l \le n\}.$$

Throughout this thesis1, we will consistently make use of the following assumptions:

Assumption 1 *Each function* $f_{ij}(z)$, $(ij = 11, 12, \cdots, mn)$ *satisfies the Lipschitz condition, i.e., there is a constant* $L_{ij} > 0$ *such that* $|f_{ij}(z_1) - f_{ij}(z_2)| \leq L_{ij}|z_1 - z_2|$ *for all* $z_1, z_2 \in \mathbb{R}$.

Assumption 2 *Each activation function is bounded, i.e., there is a constant* $M_{ij} > 0$ *such that* $|f_{ij}(z)| \leq M_{ij}$ *for all* $u \in \mathbb{R}$.

To synchronize with the master system (3.1), we have incorporated the following slave system subject to the hybrid controller $u_{ij}(t)$:

$$\frac{dy_{ij}(t)}{dt} = -\alpha_{ij}(t)y_{ij}(t) - \sum_{C_{hl}\in N_r(i,j)} C_{ij}^{hl}(t)f_{ij}\big(y_{hl}(t-\gamma_{hl}(t))\big)y_{ij}(t) + I_{ij}(t) + u_{ij}(t), \quad (3.2)$$

where the hybrid control will be defined later.

Based on master-slave systems (3.1) and (3.2) subject to the hybrid controller (3.4), the dynamics of the error system has been depicted with error state $e_{ij}(t) = y_{ij}(t) - x_{ij}(t)$ as in the following form:

$$\begin{cases} \dot{e}_{ij}(t) = & -\alpha_{ij}(t)e_{ij}(t) - \sum\limits_{C_{hl}\in N_r(i,j)} C_{ij}^{hl}(t)f_{ij}\Big(y_{hl}\big(t-\gamma_{hl}(t)\big)\Big)y_{ij}(t) \\ & + \sum\limits_{C_{hl}\in N_r(i,j)} C_{ij}^{hl}(t)f_{ij}\Big(x_{hl}\big(t-\gamma_{hl}(t)\big)\Big)x_{ij}(t) + V_{ij}(t), \\ e_{ij}(t_k^+) = e_{ij}(t_k^-) - q_{ij}e_{ij}(t_k^-), & t = t_k, (i,j) \in \mathcal{D}(t_k). \end{cases} \quad (3.3)$$

Here, the hybrid controller $u_{ij}(t)$ is assembled in the following impulsive switching mode:

$$u_{ij}(t) = \begin{cases} V_{ij}(t), \\ \sum_{k=0}^{\infty} -q_{ij}e_{ij}(t)\delta(t-t_k), \quad t = t_k, (i,j) \in \mathcal{D}(t_k), \end{cases} \quad (3.4)$$

such that
$$V_{ij}(t) = \begin{cases} \Big(-\sum\limits_{C_{hl}\in N_r(i,j)} C_{ij}^{hl}(t)M_{ij}|e_{ij}(t)| - \epsilon \\ -L_{ij}K_0 \sum\limits_{C_{hl}\in N_r(i,j)} \overline{C_{ij}^{hl}}|e_{hl}\big(t-\gamma_{hl}(t)\big)|\Big) sgn\big(e_{ij}(t)\big), & t \in [t_{k-1}, t_k), \\ 0, & t = t_k, (i,j) \notin \mathcal{D}(t_k), \end{cases}$$
and $q_{ij} \in (0,1)$ is the impulse gain; $\delta(\cdot)$ is dirac delta function; ϵ is a positive constant; the

impulse instant sequence $\{t_k\}_{k=1}^{\infty}$ satisfies $0 = t_0 < t_1 < t_2 < \cdots < t_k$, $\lim_{k\to\infty} t_k = +\infty$; the set of pinned nodes at $t = t_k$ denoted as $\mathcal{D}(t_k) \subseteq \{(i,j) : (i,j) \in \{1,2,\cdots,n\} \times \{1,2,\cdots,m\}\}$; and the parameter K_0 will be explained later.

Remark 1 *There are several ways of defining pinning strategy, $\mathcal{D}(t_k)$. In this thesis, we apply the following strategy: at each time t_k errors of all states are calculated and rearranged in decreasing order. Then we choose the first c states and apply impulsive control. The constant c is determined by the pinning ratio parameter, η_k.*

To confirm the required synchronization criteria, we have considered the following definition and the assumption:

Definition 8 *(28)The pinning ratio at time $t = t_k$ is given by $\dfrac{\sum_{ij\in\mathcal{D}(t_k)}|e_{ij}(t_k^-)|}{\sum_{k=1}^{N}|e_{ij}(t_k^-)|} = \eta_k$. This ratio indicates the portion of nodes in the desired error network influenced by pinning at the specified time.*

Assumption 3 *There exists positive constants $\theta, \overline{\theta}$ such that $\theta \leq t_{k+1} - t_k \leq \overline{\theta}$ for all $k \in \mathbb{Z}^+$.*

Remark 2 *One can easily obtain T_a and N_0 from (1) if θ and $\overline{\theta}$ are given.*

The following lemma is a modified version of the Lemma 3.1 from the (68).

Lemma 2 *Suppose that Assumptions (1), (2) and (3) are satisfied. Let θ from the Assumption (3) satisfy the inequality $\overline{C}\theta M < 1$, where $M = \max_{i,j} M_{ij}$ and $\overline{C} = \max_{i,j} \sum_{C_{hl}\in N_r(i,j)} C_{ij}^{hl}$. If there exists a positive integer H_0 satisfying the inequality*

$$\overline{C}\theta\left(M + \frac{2L(H_0 + \theta\overline{L})}{1 - C\theta M}\right) < 1,$$

then the solution $x_{ij}(t)$ on the interval $[t_k, t_{k+1})$ is unique.

Proof. Denote Λ as a set of continuous functions $x(t) = \{x_{ij}(t)\}$, $i = 1, 2, \cdots, m$ and $j = 1, 2, \cdots, n$ on $[t_k - \gamma, t_{k+1})$ such that $x_{ij}(t) = \phi(t), t \in [-\gamma, 0]$ and $||x||_1 \leq K_0$, where $||x||_1 = \max_{t \in [t_k, t_{k+1}]} ||x(t)||$ and $K_0 = \dfrac{L(H_0 + \theta \overline{L})}{1 - C\theta M}$. Define an operator Π on Λ such that

$$(\Pi x(t))_{ij} = \begin{cases} \phi(t-\sigma), & t \in (\sigma - \gamma, \sigma), \\ e^{-\alpha_{ij}(t-\sigma)}\phi_{ij}(0) - \int_\sigma^t e^{-\alpha_{ij}(t-s)}\Big[I_{ij}(s) & \\ + \sum\limits_{C_{hl} \in N_r(i,j)} C_{ij}^{hl} f(x_{hl}(s - \gamma_{hl}(s))))x_{ij}(s)\Big] ds, & t \in [\sigma, t_{k+1}), \end{cases}$$

where σ is a positive constant, and $\gamma = \max_{hl,t} |\gamma_{hl}(t)|$. From the definition, we can easily confirm that $|(\Pi x(t))_{ij}| \leq H_0 + (MK_0 \sum_{C_{hl} \in N_r(i,j)} C_{ij}^{hl} + \overline{I})\theta$ for $t \in [\sigma, t_{k+1})$. Thus, the inequality $||\Pi x||_1 \leq H_0 + (\overline{C}MK_0 + \overline{I})\theta = K_0$ holds. Therefore, $\Pi(\Lambda) \subseteq \Lambda$.

Now, assume that $x(t) = \{x_{ij}(t)\}$ and $z(t) = \{z_{ij}(t)\}$ belong to Λ. Then, for $t \in [\sigma, t_{k+1})$, one has

$$\begin{aligned} (\Pi x(t))_{ij} - (\Pi z(t))_{ij} \leq & \int_\sigma^t e^{-\alpha_{ij}(t-s)} \sum_{C_{hl} \in N_r(i,j)} C_{ij}^{hl} \Big| f\Big(x_{hl}\big(s - \gamma_{hl}(s)\big)\Big)\Big| \Big| x_{ij}(s) - z_{ij}(s)\Big| ds \\ & + \int_\sigma^t e^{-\alpha_{ij}(t-s)} \sum_{C_{hl} \in N_r(i,j)} C_{ij}^{hl} \Bigg| \bigg(f\Big(x_{hl}\big(s - \gamma_{hl}(s)\big)\big) \\ & - f\Big(z_{hl}\big(s - \gamma_{hl}(s)\big)\Big)\bigg)\Bigg| \Big| x_{ij}(s)\Big| ds \\ \leq & \theta(M + 2K_0 I)||x - z||_1 \sum_{C_{hl} \in N_r(i,j)} C_{ij}^{hl}. \end{aligned}$$

Hence, the inequality $||\Pi x - \Pi z||_1 \leq \overline{C}\theta(M + 2K_0 I)||x - z||_1$ is valid. As $\overline{C}\theta(M + 2K_0 I) = \overline{C}\theta\left(M + 2I\dfrac{H_0 + \theta I}{1 - C\theta M}\right) < 1$, the operator Π exhibits contraction property. It follows that a unique solution for $x(t)$ exists on the interval $[\sigma, t_{k+1})$.

Lemma 3 *Suppose the Assumptions 1 and 2 hold. Let us define the Lyapunov function as* $V(t) = \sum_{i,j} |e_{ij}(t)|$ *such that the error dynamics* $e_{ij}(t) = y_{ij}(t) - x_{ij}(t)$*, in which* $x_{ij}(t)$

revealed by Lemma 2. For $t \in [t_k, t_{k+1})$, *the following inequality holds:*

$$\begin{aligned} D^+V(t) &\leq \sum_{i,j} \Bigg[\sum_{C_{hl} \in N_r(i,j)} C_{ij}^{hl}(t) M_{ij} \big| e_{ij}(t) \big| + \sum_{C_{hl} \in N_r(i,j)} K_0 \overline{C_{ij}^{hl}} L_{ij} \Big| e_{hl}\big(t - \gamma_{hl}(t)\big) \Big| \\ &\quad + u_{ij}(t) sgn\big(e_{ij}(t)\big) \Bigg], \end{aligned} \tag{3.5}$$

where the K_0 *is as in Lemma 2.*

Proof. Let us find the derivative of $V(t) = \sum_{i,j} |e_{ij}(t)|$ along with the solution state $e_{ij}(t)$, that is,

$$
\begin{aligned}
D^+V(t) =& \sum_{i,j} sgn\big(e_{ij}(t)\big)\dot{e}_{ij}(t) \\
=& \sum_{i,j} sgn\big(e_{ij}(t)\big)\Bigg[-\alpha_{ij}(t)e_{ij}(t) - \sum_{C_{hl}\in N_r(i,j)} C_{ij}^{hl}(t) f_{ij}\Big(y_{hl}\big(t-\gamma_{hl}(t)\big)\Big)y_{ij}(t) \\
&+ \sum_{C_{hl}\in N_r(i,j)} C_{ij}^{hl}(t) f_{ij}\Big(x_{hl}\big(t-\gamma_{hl}(t)\big)\Big)x_{ij}(t) + u_{ij}(t)\Bigg] \\
=& \sum_{i,j} sgn\big(e_{ij}(t)\big)\Bigg[-\alpha_{ij}(t)e_{ij}(t) - \sum_{C_{hl}\in N_r(i,j)} C_{ij}^{hl}(t) f_{ij}\big(y_{hl}\big(t-\gamma_{hl}(t)\big)\big)e_{ij}(t) \\
&- \sum_{C_{hl}\in N_r(i,j)} C_{ij}^{hl}(t)\bigg(f_{ij}\Big(y_{hl}\big(t-\gamma_{hl}(t)\big)\Big) - f_{ij}\Big(x_{hl}\big(t-\gamma_{hl}(t)\big)\Big)\bigg)x_{ij}(t) + u_{ij}(t)\Bigg] \\
\leq& \sum_{i,j}\Bigg[\sum_{C_{hl}\in N_r(i,j)} C_{ij}^{hl}(t)\bigg|f_{ij}\Big(y_{hl}\big(t-\gamma_{hl}(t)\big)\Big) - f_{ij}(x_{hl}\Big(t-\gamma_{hl}(t)\big)\Big)\bigg|\big|x_{ij}(t)\big| \\
&- \alpha_{ij}(t)\big|e_{ij}(t)\big| \sum_{C_{hl}\in N_r(i,j)} C_{ij}^{hl}(t)\bigg|f_{ij}\Big(y_{hl}\big(t-\gamma_{hl}(t)\big)\Big)\bigg|\big|e_{ij}(t)\big| + u_{ij}(t)sgn\big(e_{ij}(t)\big)\Bigg] \\
\leq& \sum_{i,j}\Bigg[-\alpha_{ij}(t)\big|e_{ij}(t)\big| + \sum_{C_{hl}\in N_r(i,j)} C_{ij}^{hl}(t)M_{ij}\big|e_{ij}(t)\big| \\
&+ K_0 \sum_{C_{hl}\in N_r(i,j)} C_{ij}^{hl}(t)L_{ij}\Big|e_{hl}\big(t-\gamma_{hl}(t)\big)\Big| + u_{ij}(t)sgn\big(e_{ij}(t)\big)\Bigg] \\
\leq& \sum_{i,j}\Bigg[\sum_{C_{hl}\in N_r(i,j)} C_{ij}^{hl}(t)M_{ij}\big|e_{ij}(t)\big| + \sum_{C_{hl}\in N_r(i,j)} K_0\overline{C_{ij}^{hl}}L_{ij}\Big|e_{hl}\big(t-\gamma_{hl}(t)\big)\Big| \\
&+ u_{ij}(t)sgn\big(e_{ij}(t)\big)\Bigg]
\end{aligned}
$$

That completes the proof.

The next lemma is a modified version of the comparison system from (69).

Lemma 4 *For error dynamics* (3.3), *if there exists a function* $V(u_{ij}(t)) \in \nu_0$ *such that* $V(0)$ *is continuous function on* $[-\overline{\gamma}, 0]$, *and if the following is true for some* γ *and* $\mu \in (0,1)$*:*

$$\begin{cases} \dot{v}(t) = -\epsilon, & t \neq t_k, \\ v(t_k^+) = \mu v(t_k^-), & t = t_k, \\ v(0) = V(0), & t \in [-\overline{\gamma}, 0], \end{cases} \tag{3.6}$$

here $\epsilon > 0$ *and* t_k *is a impulse instant sequence in hybrid controller* (3.6), *then following inequality holds*

$$v(t) \leq \left(\mu^{-N_0} v(0) - \epsilon \mu^{N_0} \frac{T_a}{\ln \mu}\right) \mu^{\frac{t}{T_a}} + \epsilon \mu^{N_0} \frac{T_a}{\ln \mu}.$$

Proof. By applying the theory of ordinary differential equation to (3.6) for $t \in [0, t_1)$, we obtain the following:

$$v(t) = v(0) - \int_0^t \epsilon ds \text{ and } v(t_1^-) = v(0) - \int_0^{t_1} \epsilon ds.$$

For $t \in [t_1, t_2)$,

$$v(t) = v(t_1) - \int_0^t \epsilon ds \text{ and } v(t_2^-) = v(t_1) - \int_0^{t_2} \epsilon ds.$$

At $t = t_1$,

$$v(t_1) = \mu v(t_1^-) = \mu\left(v(0) - \int_0^{t_1} \epsilon ds\right) = \mu v(0) - \mu \int_0^{t_1} \epsilon ds.$$

For $t \in [t_2, t_3)$,

$$v(t) = v(t_2) - \int_0^t \epsilon ds \text{ and } v(t_3^-) = v(t_2) - \int_0^{t_3} \epsilon ds.$$

At $t = t_2$,

$$v(t_2) = \mu v(t_2^-) = \mu\left(v(t_1) - \int_0^{t_2} \epsilon ds\right) = \mu v(t_1) - \mu \int_0^{t_2} \epsilon ds$$

$$= \mu\bigg(\mu v(0) - \mu\int_0^{t_1}\epsilon ds\bigg) - \mu\int_0^{t_2}\epsilon ds = \mu^2 v(0) - \mu^2\int_0^{t_1}\epsilon ds - \mu\int_0^{t_2}\epsilon ds.$$

Then for $t \in [0, t_{k+1})$, by mathematical induction one can obtain:

$$\begin{aligned} v(t) &= \mu^k v(0) - \mu^k \int_0^{t_1}\epsilon ds - \mu^{k-1}\int_{t_1}^{t_2}\epsilon ds - \cdots \\ &- \mu\int_{t_{k-1}}^{t_k}\epsilon ds - \int_{t_k}^{t}\epsilon ds \\ &= \mu^{N(t,0)}v(0) - \epsilon\int_0^t \mu^{N(t,s)}ds. \end{aligned}$$

By using definition (1) and $\mu \in (0,1)$ following inequality is obtained:

$$\begin{aligned} v(t) &\leq \mu^{\frac{t}{T_a}-N_0}v(0) - \epsilon\int_0^t \mu^{\frac{t-s}{T_a}-N_0} \\ &= (\mu^{-N_0}v(0) - \epsilon\mu^{N_0}\frac{T_a}{\ln\mu})\mu^{\frac{t}{T_a}} + \epsilon\mu^{N_0}\frac{T_a}{\ln\mu}. \end{aligned}$$

This completes the proof.

3.1 Main results

In this section, we endeavor to demonstrate the finite-time synchronization between the master system (3.1) and the slave system (3.2). This assertion will be substantiated through a series of case studies, showcasing the effectiveness of the proposed hybrid controller (3.4).

Theorem 4 *Suppose that Assumptions* (1), (2) *and* (3) *are satisfied. Then the error system* (3.3) *will synchronize in finite time with settling time* T_1 *under control* (3.4). *Here*

$$T_1 = \frac{T_a}{\ln\mu_1}\ln\left(\frac{\epsilon T_a\mu_1^{2N_o}}{\epsilon T_a\mu_1^{2N_o} - V(0)\ln\mu_1}\right), \tag{3.7}$$

$\mu = 1 - q\eta_k$, *and* $q = \max_{ij}(q_{ij})$.

Proof. Choose the Lyapunov function to be $V(t) = \sum\limits_{i,j} |e_{ij}(t)|$. Then from Lemma (3) for $t \in [t_{k-1}, t_k)$ we have

$$D^+V(t) \leq \sum_{i,j} \Bigg[\sum_{C_{hl} \in N_r(i,j)} C_{ij}^{hl}(t) M_{ij} \big|e_{ij}(t)\big| + \sum_{C_{hl} \in N_r(i,j)} K_0 \overline{C_{ij}^{hl}} L_{ij} \Big|e_{hl}\big(t - \gamma_{hl}(t)\big)\Big| + u_{ij}(t) sgn\big(e_{ij}(t)\big) \Bigg] = -\epsilon.$$

For $t = t_k$ we have

$$\begin{aligned} V(t_k^+) = & \sum_{ij} |e_{ij}(t_k^+)| = \sum_{ij \in D(t_k)} |e_{ij}(t_k^+)| + \sum_{ij \notin D(t_k)} |e_{ij}(t_k^+)| \\ \leq & \sum_{ij \in D(t_k)} (1-q)|e_{ij}(t_k^-)| + \sum_{ij \notin D(t_k)} |e_{ij}(t_k^-)| \\ = & (1-q) \sum_{ij \in D(t_k)} |e_{ij}(t_k^-)| + \sum_{ij \notin D(t_k)} |e_{ij}(t_k^-)| \\ = & (1-q)\eta_k \sum_{ij} |e_{ij}(t_k^-)| + (1-\eta_k) \sum_{ij} |e_{ij}(t_k^-)| \\ = & \big((1-q)\eta_k + (1-\eta_k)\big) \sum_{ij} |e_{ij}(t_k^-)| = (1 - q\eta_k) V(t_k^-) = \mu_1 V(t_k^-). \end{aligned}$$

Now we have the comparison system, which is based aforementioned results

$$\begin{cases} \dot{v}(t) = -\epsilon, & t \neq t_k, \\ v(t_k^+) = \mu_1 v(t_k^-), & t = t_k, \\ v(0) = V(0), & t \in [-\overline{\gamma}; 0]. \end{cases}$$

This means that if $0 \leq V(t) \leq v(t)$ for $-\overline{\gamma} \leq t \leq 0$ then $V(t) \leq v(t)$ for all $t > 0$. By Lemma (4) the solution for this comparison system is as follows:

$$v(t) \leq (\mu_1^{-N_0} v(0) - \epsilon \mu_1^{N_0} \frac{T_a}{\ln \mu_1}) \mu_1^{\frac{t}{T_a}} + \epsilon \mu_1^{N_0} \frac{T_a}{\ln \mu_1}.$$

Since $0 < \mu_1 < 1$, $\ln \mu_1 < 0$. Then we can see that $(\mu_1^{-N_0} v(0) - \epsilon \mu_1^{N_0} \frac{T_a}{\ln \mu_1}) > 0$ and $\epsilon \mu_1^{N_0} \frac{T_a}{\ln \mu_1} < 0$. Since $V(0) > 0$ there is $T_1 \in (0, \infty)$ such that the right-hand side of the equation above will be equal to 0, and this value is equal to $T_1 = \frac{T_a}{ln \mu_1} \cdot ln(\frac{\epsilon T_a \mu_1^{2N_o}}{\epsilon T_a \mu_1^{2N_o} - V(0) ln \mu_1})$.

Remark 3 *Hybrid control gives finite time synchronization, however, this can be achieved with a slightly different control. The hybrid control consists of three parts: feedback, pinning, and impulsive control. Now the proof that finite-time synchronization could be achieved with feedback control only will be given.*

Let the feedback control be as follows

$$u_{ij}(t) = \left[- \sum_{C_{hl} \in N_r(i,j)} C_{ij}^{hl}(t) M_{ij} \big| e_{ij}(t) \big| - L_{ij} K_0 \sum_{C_{hl} \in N_r(i,j)} \overline{C_{ij}^{hl}} \Big| e_{hl}\big(t - \gamma_{hl}(t)\big) \Big| - \epsilon \right] sgn(e_{ij}(t)). \tag{3.8}$$

Theorem 5 *Suppose that Assumptions* (1), (2) *and* (3) *are satisfied. Then the error system* (3.3) *will synchronize in finite time with settling time T_2 under the control* (3.8), *where* $T_2 = \frac{V(0)}{\epsilon}$ *and* $V(0) = \sum\limits_{i,j} |e_{ij}(0)|$.

Proof. Choose the Lyapunov function to be $V(t) = \sum\limits_{i,j} |e_{ij}(t)|$. Then from Lemma (3) we get that

$$\begin{aligned} D^+V(t) \leq \ & \sum_{i,j} \Bigg[\sum_{C_{hl} \in N_r(i,j)} C_{ij}^{hl}(t) M_{ij} \big| e_{ij}(t) \big| + \sum_{C_{hl} \in N_r(i,j)} K_0 \overline{C_{ij}^{hl}} L_{ij} \Big| e_{hl}\big(t - \gamma_{hl}(t)\big) \Big| \\ & + u_{ij}(t) sgn\big(e_{ij}(t)\big) \Bigg] = -\epsilon, \end{aligned}$$

Based on this inequality and initial conditions, we have the comparison system

$$\begin{cases} \dot{v}(t) = -\epsilon, & t \in [-\overline{\gamma}; 0], \\ v(0) = V(0), & k \in N. \end{cases}$$

By using ordinary differential equation theory, we have $v(t) = v(0) - \int_0^t \epsilon ds = v(0) - \epsilon t$. Since $v(0) > 0$ and $\epsilon > 0$, there is $T_2 \in (0, +\infty)$ such that $v(t) = 0$ and $T_2 = \frac{\epsilon}{V(0)}$.

Remark 4 *To do a comprehensive comparison analysis third control, impulsive feedback control, needs to be introduced. This control consists of only impulsive control and feedback control, which means, at time t_k control will be applied to all nodes.*

Let impulsive feedback control be defined as

$$u_{ij}(t) = \begin{cases} \sum_{k=0}^{\infty} -q_{ij} e_{ij}(t)\delta(t-t_k), & t = t_k, \\ \Big(- \sum\limits_{C_{hl}\in N_r(i,j)} C_{ij}^{hl}(t) M_{ij} \big|e_{ij}(t)\big| - \epsilon & \\ -L_{ij}K_0 \sum\limits_{C_{hl}\in N_r(i,j)} \overline{C_{ij}^{hl}} |e_{hl}\big(t-\gamma_{hl}(t)\big)| \Big) sgn\big(e_{ij}(t)\big), & t \in [t_{k-1}, t_k). \end{cases} \tag{3.9}$$

Theorem 6 *Suppose that Assumptions* (1), (2) *and* (3) *are satisfied. Then the error system* (3.3) *will synchronize in finite time with settling time* T_3 *under the control* (3.9). *Here*

$$T_3 = \frac{T_a}{\ln \mu_2} \ln\left(\frac{\epsilon T_a \mu_2^{2N_o}}{\epsilon T_a \mu_2^{2N_o} - V(0)\ln \mu_2} \right),$$

$\mu_2 = 1 - q,$ *and* $q = \max_{ij}(q_{ij})$.

Proof. Choose the Lyapunov function to be $V(t) = \sum\limits_{i,j} |e_{ij}(t)|$. Then from Lemma (3) for $t \in [t_{k-1}, t_k)$ we have

$$\begin{aligned} D^+V(t) \leq \ & \sum_{i,j}\Bigg[\sum_{C_{hl}\in N_r(i,j)} C_{ij}^{hl}(t) M_{ij} \big|e_{ij}(t)\big| + \sum_{C_{hl}\in N_r(i,j)} K_0 \overline{C_{ij}^{hl}} L_{ij} \Big| e_{hl}\big(t-\gamma_{hl}(t)\big)\Big| \\ & + u_{ij}(t) sgn\big(e_{ij}(t)\big)\Bigg] = -\epsilon. \end{aligned}$$

For $t = t_k$ we have

$$V(t_k^+) = \sum_{ij} |e_{ij}(t_k^+)| \leq \sum_{ij} \big|(1-q) e_{ij}(t_k^-)\big| = (1-q) \sum_{ij} \big|e_{ij}(t_k^-)\big| = \mu_2 V(t_k^-).$$

Now we have the comparison system, which is based on the aforementioned results

$$\begin{cases} \dot{v}(t) = -\epsilon, & t \neq t_k, \\ v(t_k^+) = \mu_2 v(t_k^-), & t = t_k, \\ v(0) = V(0), & t \in [-\overline{\gamma}; 0]. \end{cases} \tag{3.10}$$

This means that if $0 \leq V(t) \leq v(t)$ for $-\overline{\gamma} \leq t \leq 0$ then $V(t) \leq v(t)$ for all $t > 0$. By Lemma 3, the solution for this comparison system is as follows:

$$v(t) \leq \left(\mu_2^{-N_0} v(0) - \epsilon \mu_2^{N_0} \frac{T_a}{\ln \mu_2}\right) \mu_2^{\frac{t}{T_a}} + \epsilon \mu_2^{N_0} \frac{T_a}{\ln \mu_2}.$$

Since $0 < \mu_2 < 1$, $\ln \mu_2 < 0$, we can see that $\left(\mu_2^{-N_0} v(0) - \epsilon \mu_2^{N_0} \frac{T_a}{\ln \mu_2}\right) > 0$ and $\epsilon \mu_2^{N_0} \frac{T_a}{\ln \mu_2} < 0$. There exists $T_3 \in (0, \infty)$ such that the right-hand side of the equation above will be equal to 0, and this value is equal to $T_3 = \frac{T_a}{ln \mu_2} \ln \left(\frac{\epsilon T_a \mu_2^{2N_o}}{\epsilon T_a \mu_2^{2N_o} - V(0) ln \mu_2} \right)$.

Remark 5 *One can notice that the settling times of all controls are expressed in terms of initial values. The following theorem provides the proof as well as the necessary and sufficient conditions for hybrid and impulsive feedback control to outperform classical feedback control.*

Theorem 7 *Suppose that the average impulse interval is less than T_a and that Assumptions 1, 2 and 3 are satisfied. Then the inequality $T_3 < T_1 < T_2$ holds if the condition $\epsilon < \frac{v(0)}{x_0}$ true. Here $x_0 = \left[W_{-1}(-\frac{\mu^{2N_0}}{e^{\mu^{2N_0}}}) + \mu^{2N_0}\right] \frac{T_a}{ln \mu}$, $\mu = max\{\mu_1, \mu_2\}$ and W_{-1} is the -1 branch of the Lambert function.*

Proof. Let us assume that $T = max\{T_1, T_3\}$, it gives

$$\begin{aligned} T &= \frac{T_a}{\ln \mu} \ln \left(\frac{\epsilon T_a \mu^{2N_o}}{\epsilon T_a \mu^{2N_o} - V(0) \ln \mu} \right) = \frac{T_a}{\ln \mu} \ln \left(\frac{T_a \mu^{2N_o}}{T_a \mu^{2N_o} - \frac{V(0)}{\epsilon} \ln \mu} \right) \\ & \frac{T_a}{\ln \mu} \ln \left(\frac{T_a \mu^{2N_o}}{T_a \mu^{2N_o} - T_2 \ln \mu} \right), \end{aligned}$$

which means that T can be expressed as a function of T_2 and parameters $\mu \in (0,1), T_a > 0, N_0 \in N$. Now, we can compare T and T_2. First, let $T_2 = x$ and $T = y$, then we will have y as a function of x and some parameters, namely $y = f(x, \mu, N_0, T_a)$:

$$y = \frac{T_a}{\ln \mu} \ln \left(\frac{T_a \mu^{2N_o}}{T_a \mu^{2N_o} - x \ln \mu} \right). \tag{3.11}$$

Several steps are needed to compare x and y.

1. Do functions $y_1 = x$ and $y_2 = f(x, \mu, N_0, T_a)$ intersect?

2. If so, what is the exact value of the intersection point?

As we answer these questions, we will compare x and y. The first thing to note is that x, y are settling times, therefore we are looking for only $x, y > 0$. In addition, one can easily verify that there is an intersection at $x = 0$. Since this intersection gives no information, we need a non-zero intersection point. To find this, the derivatives of the above-mentioned two functions are used: $\frac{dy_1}{dx} = 1$ and $\frac{dy_2}{dx} = \frac{T_a}{T_a \mu^{2N_o} - x \ln \mu}$. Then by taking limits of the derivatives, $x \to 0^+$ and $x \to +\infty$ we have:

$$\lim_{x \to 0^+} \frac{dy_1}{dx} = 1, \quad \lim_{x \to 0^+} \frac{dy_2}{dx} = \frac{1}{\mu^{2N_0}}, \quad \lim_{x \to 0^+} \frac{dy_1}{dx} < \lim_{x \to 0^+} \frac{dy_2}{dx},$$
$$\lim_{x \to +\infty} \frac{dy_1}{dx} = 1, \quad \lim_{x \to +\infty} \frac{dy_2}{dx} = 0, \quad \lim_{x \to +\infty} \frac{dy_1}{dx} > \lim_{x \to +\infty} \frac{dy_2}{dx}.$$

From here, we can observe that at 0^+ y_2 is greater than y_1, which means T is greater than T_2, and as x goes to infinity, y_1 is greater than y_2. Therefore, at least one intersection exists between y_1 and y_2 for $x \in (0, +\infty)$.
The second derivative of y_2 is as follows:

$$\frac{d}{dx}\left(\frac{dy_2}{dx}\right) = \frac{T_a \ln \mu}{\left(T_a \mu^{2N_o} - x \ln \mu\right)^2}.$$

$\ln \mu < 0$ since $\mu \in (0, 1)$, T_a is a positive constant, and the denominator is always positive: $y_2'' < 0$, or the function y_2 is concave down for all $x > 0$. Therefore, we have only one non-zero intersection between y_1 and y_2, let's define it as x_0. From previously obtained limits we can claim that if $x \in (0, x_0)$ then $T > T_2$ and $T < T_2$, if otherwise.

To find the intersection point, we solve the following equation: $y_1 = y_2$. By rearranging the terms from 3.11 , we get $a = x\frac{\ln \mu}{T_a}$ and $b = \mu^{2N_0}$. Then make a substitution as $u = a - b \to a = u + b$, to get $e^u u = -\frac{b}{e^b}$. One needs to solve for u, which cannot be solved explicitly, so we use a special function called Lambert W function. By applying the -1 branch of Lambert W function, we have $u = W_{-1}\left(-\frac{b}{e^b}\right)$. After, substitute back to the original parameters to find x_0:

$$x_0 = \left(W_{-1}\left(-\frac{\mu^{2N_0}}{e^{\mu^{2N_0}}} \right) + \mu^{2N_0} \right) \frac{T_a}{\ln \mu}.$$

$T_2 > x_0$ implies that $T < T_2$. After substituting $T_2 = \frac{V(0)}{\epsilon}$ we will have necessary conditions for $T < T_2$, which is $\epsilon < \frac{v(0)}{x_0}$. Therefore, for $0 < \epsilon < \frac{v(0)}{x_0}$, feedback impulsive, and hybrid controls do faster synchronization than feedback control. Furthermore, by using the first derivative test (3.11) with respect to μ, one can easily proof that if $\mu_2 \leq \mu_1$, then $T_3 \leq T_1$.

Chapter 4

Numerical Example

In this section, numerical simulations are given to support the theoretical results. All simulations were performed using the built-in function 'dde23' in the MATLAB software. Consider a 2×3 system with $t_0 \in [-0.5, 0]$ and with the following parameters:

$$\begin{pmatrix} x_{11}(t_0) & x_{12}(t_0) & x_{13}(t_0) \\ x_{21}(t_0) & x_{22}(t_0) & x_{23}(t_0) \end{pmatrix} = \begin{pmatrix} -0.025 & 0.036 & -0.014 \\ 0.012 & 0.042 & 0.042 \end{pmatrix}$$

$$\begin{pmatrix} y_{11}(t_0) & y_{12}(t_0) & y_{13}(t_0) \\ y_{21}(t_0) & y_{22}(t_0) & y_{23}(t_0) \end{pmatrix} = \begin{pmatrix} 0.05 & 0.08 & 0.12 \\ -0.3 & -0.12 & -0.12 \end{pmatrix}$$

$$\begin{pmatrix} C_{11}(t) & C_{12}(t) & C_{13}(t) \\ C_{21}(t) & C_{22}(t) & C_{23}(t) \end{pmatrix} = \begin{pmatrix} 0.001 & 0.002 & 0.003 \\ 0.004 & 0.005 & 0.001 \end{pmatrix}$$

$$\begin{pmatrix} \gamma_{11}(t) & \gamma_{12}(t) & \gamma_{13}(t) \\ \gamma_{21}(t) & \gamma_{22}(t) & \gamma_{23}(t) \end{pmatrix} = \begin{pmatrix} 0.2 & 0.5 & 0.2 \\ 0.5 & 0.5 & 0.3 \end{pmatrix}$$

$$\begin{pmatrix} \alpha_{11}(t) & \alpha_{12}(t) & \alpha_{13}(t) \\ \alpha_{21}(t) & \alpha_{22}(t) & \alpha_{23}(t) \end{pmatrix} = \begin{pmatrix} 0.00086385 & 0.00056385 & 0.00066385 \\ 0.00046385 & 0.00046385 & 0.00046385 \end{pmatrix}$$

$$\begin{pmatrix} I_{11}(t) & I_{12}(t) & I_{13}(t) \\ I_{21}(t) & I_{22}(t) & I_{23}(t) \end{pmatrix} = \begin{pmatrix} 0.0005 & -0.0003 & -0.0003 \\ 0.0001 & -0.0001 & 0.0001 \end{pmatrix}$$

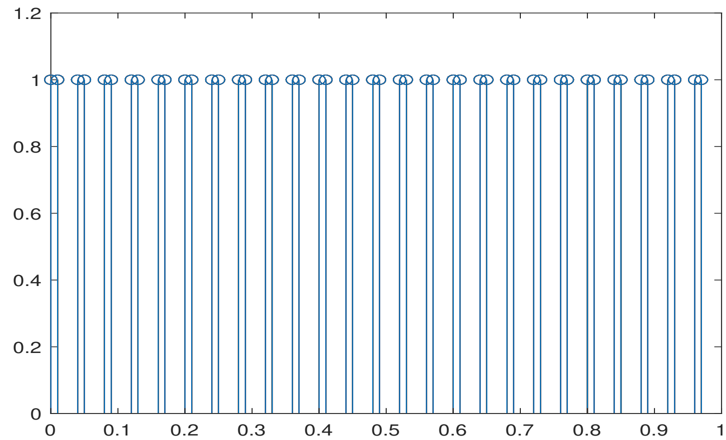

Figure 4-1: The impulse instant sequence $\{t_k\}_{k=1}^{\infty}$.

The activation function is chosen as $f_{ij}(x) = 0.125|x+0.1| - 0.125|x-0.7|$. For this activation function, the Lipschitzian constant and maximum of the function are given by $L_{ij} = 1$ and $M_{ij} = 0.1$. With these parameters, the state trajectories for the master-slave system without the controller are obtained and shown in Fig. 4-2. For the convenience of the reader, this and the following graphs display the behavior for the error state,
$e_{ij}(t) = y_{ij}(t) - x_{ij}(t)$.

To get simulations of (3.8) with feedback control set $\epsilon = 0.5$. The error system with feedback control is shown in Fig. 4-3.

For the impulse instant sequence t_k, which is used in impulsive feedback and hybrid impulsive pinning control, the parameters in Assumption 3 are chosen as $\theta = \frac{1}{52}$ and $\overline{\theta} = \frac{1}{48}$. One can easily calculate the values of T_a and N_0, which are 0.02 and 2 respectively. The Fig. 4-1 shows the impulse control sequence.

The strategy of pinning was explained in the Remark 1. The parameters for pinning ratio and impulse gain are chosen as follows: $q_{ij} = 0.9$, $\eta_k = 0.5$ for all i, j and k. Recall that in impulsive feedback control, at $t = t_k$, impulses are applied to all states, not only for the part of all states with the highest error. Figs. (4-4) and (4-5) show impulsive feedback and hybrid control simulations, respectively.

In the table (4.1) computation time of each control against two different accuracy

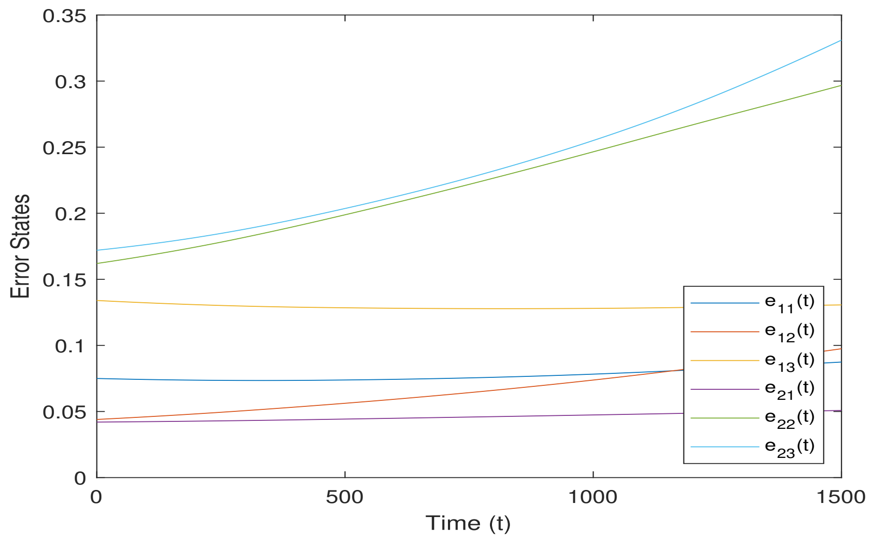

Figure 4-2: Error system (3.3) without controller does not give synchronization as errors do not tend to 0.

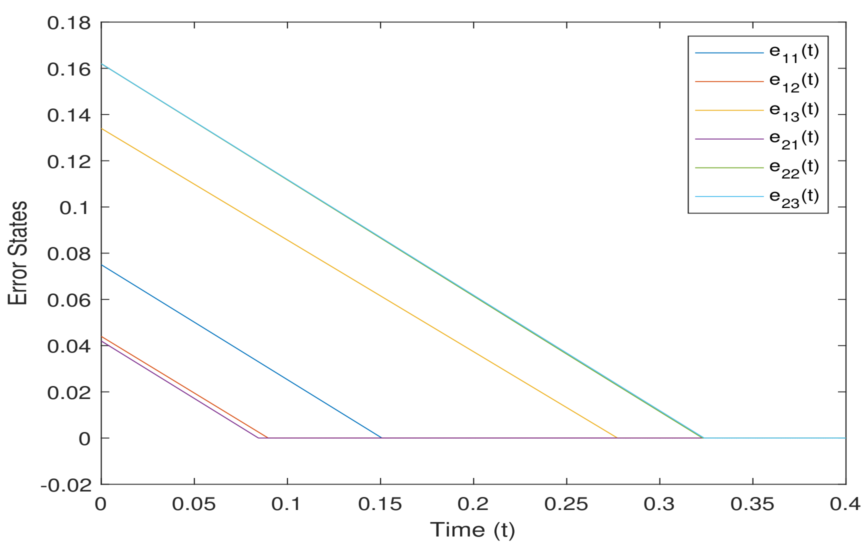

Figure 4-3: Error system (3.3) gives finite-time synchronization with feedback control (3.8) with the settling time being between 0.09 and 0.33 depending on the initial conditions.

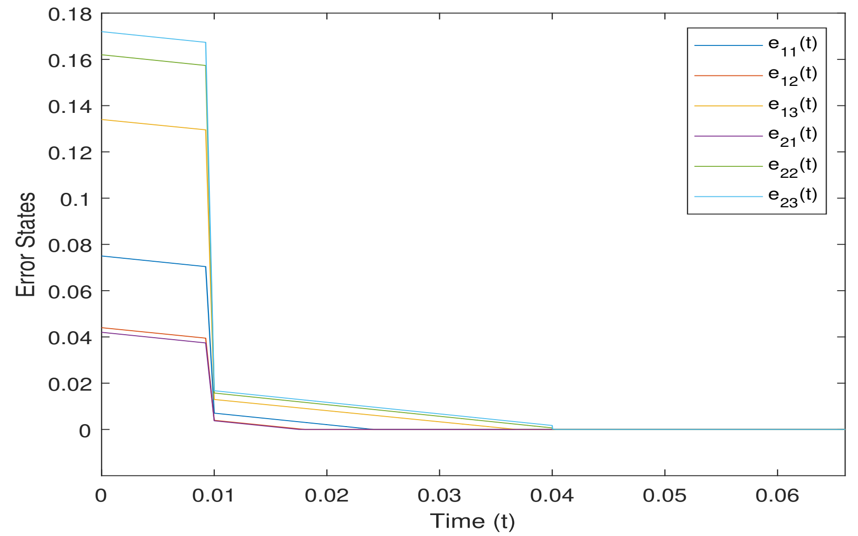

Figure 4-4: Error system (3.3) gives finite-time synchronization with impulsive feedback control (3.9) with the settling time being between 0.01 and 0.04 depending on the initial conditions.

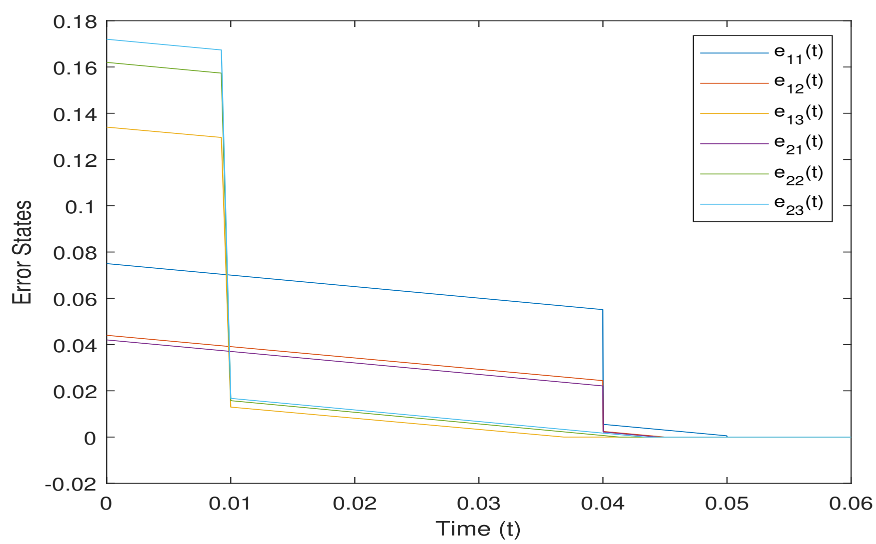

Figure 4-5: Error system (3.3) gives finite-time synchronization with impulsive feedback control (3.7) with the settling time being between 0.03 and 0.05 depending on the initial conditions.

Control type	Settling time (average)	Mesh 10^{-6}	Mesh 10^{-8}
Feedback control	0.21 sec	296 sec	~ 7.7 h
Impulsive feedback control	0.025 sec	376 sec	~ 9 h
Hybrid control	0.04 sec	314 sec	~ 8 h

Table 4.1: Computational cost of each control with two different values of accuracy

values is shown. To get appropriate values, all these simulations were done on the computer with the following characteristics: Intel Core $i9$ processor and $16GB$ RAM.

Chapter 5

Discussion

By substituting the calculated parameters from numerical simulations into the theorems, we obtain the following results:

- for feedback control: the settling time is $T_2 = 1.258$;
- for hybrid control: we get that $\mu_1 = 0.55$ and the settling time is $T_1 = 0.201$;
- for impulsive feedback control; the $\mu_2 = 0.1$ and the settling time is $T_3 = 0.123$.

By substituting values into the theorem (7), we obtain that for $\epsilon < 5.03$, hybrid and impulsive feedback control performs better than feedback control.

From Fig. (4-2) one can notice that the master-slave system (3.3) does not synchronize if control is not applied. However, the system becomes finite-time synchronized after adding one of the controllers to the slave system, regardless of the controller type. Finite-time synchronization with feedback, impulsive feedback, and hybrid impulsive pinning controls are shown in Figs. (4-3),(4-4), and (4-5), respectively. These results demonstrate that impulsive feedback control synchronizes faster than hybrid impulsive pinning control, which in turn synchronizes faster than feedback control. Furthermore, the manual calculations and the numerical simulations coincide with the obtained theoretical results, which supports the findings of comparative analysis.

It is important to point out an interesting phenomenon that can be observed in the simulations with feedback control - the synchronization rate is linear. The same situation is repeated in simulations of other controls, except for a discrete time domain. The reason for that is the parameter ϵ, which was tuned as a positive constant. In future studies, it can be changed to a time-varying variable.

Finally, in the table (4.1), the computational cost of each control is shown. In the table two different values of accuracy, or in other words, two different values of mesh are given. It was done to imitate the high dimensional system and how each control will cope with this. As predicted, a minor sacrifice in settling time results in a major gain in computation time. Therefore considering settling time and computation cost, hybrid impulsive pinning control is better than impulsive feedback and classical feedback control.

Chapter 6

Conclusion

In this thesis, we considered the finite time synchronization problem of SICNN with time-varying delays. Our main goal was to improve previous results on finite-time synchronization in terms of faster synchronization, or smaller settling time. Previously finite-time synchronization of SICNN was achieved by using feedback control. The feedback control was upgraded by adding impulses since impulsive control helps to decrease the error between the master and slave system instantaneously. However, excessive utilization of impulses leads to high control costs, which means the control will be computationally difficult. In this regard, we have strengthened control once more in order to get a consensus on better settling time and computational cost by adding pinning control. As a result, a hybrid impulsive pinning control was proposed. Therefore in order to make a qualitative comparison we considered three types of control: classical feedback control, impulsive feedback control, and a novel hybrid impulsive pinning control. Then by applying the Lyapunov function sufficient conditions to ensure finite-time synchronization for the aforementioned three types of controls were given. After, a comprehensive comparison analysis of these controls was given. The comparative analysis included the comparison of settling times of each control and proved the effectiveness of hybrid impulsive pinning control and impulsive feedback control over feedback control. The theoretical results were confirmed by numerical simulations, which consisted of manual calculations and graphs obtained using MATLAB software. Finally, a table with computational cost was obtained by using the same software. The table included the average value of settling times and execution time for two different mesh amounts of each control. This shows that hybrid control is computationally quicker than impulsive feedback control. Based on these results, we conclude that by sacrificing a small amount of settling time, control costs of the system can be decreased.

Chapter 7

Future plans

In this thesis work, we introduced that finite-time synchronization in SICNN with time-varying delays could be improved in terms of faster synchronization and less computational difficulty. In the future, this topic might be used and developed in a variety of ways. The primary examples of future study emphasis are listed below.

- *Different control strategy:* On the one hand, by applying different strategies for pinning control, computation time could be decreased once again. On the other hand, because we used constant epsilon in the hybrid impulsive pinning control, it may be changed to time-varying. After that, the obtained results could be investigated and analysed to determine the best function for the epsilon.
- *Different model:* To apply the hybrid impulsive pinning control to different models. Furthermore, a complete study of the other models with different controls might be performed. Because if the system already has impulses, impulsive control may produce significant computational difficulties or even instability.
- *Fixedtime synchronization:* Fixed-time synchronization implies that the settling time of the finite-time synchronization is bounded by a positive constant. The ability to achieve fixed-time synchronization could be researched. In addition, a comprehensive analysis of three distinct settling times of fixed-time synchronization could be done.

Chapter 8

Reference

[1] C. M. Bishop. Neural networks and their applications. *Review of Scientific Instruments*, 65(6):1803–1832, 1994.

[2] L. O. Chua and T. Roska. *Cellular neural networks and visual computing: foundations and applications*. Cambridge University Press, 2005.

[3] L. O. Chua and L. Yang. Cellular neural networks: applications. *IEEE Transactions on Circuits and Systems*, 35(10):1273–1290, 1988.

[4] L. O. Chua and L. Yang. Cellular neural networks: theory. *IEEE Transactions on Circuits and Systems*, 35(10):1257–1272, 1988.

[5] K. R. Crounse and L. O. Chua. Methods for image processing and pattern formation in Cellular Neural Networks: a tutorial. *IEEE Transactions on Circuits and Systems*, 42(10):583–601, 1995.

[6] L. Zhou. Global asymptotic stability of cellular neural networks with proportional delays. *Nonlinear Dynamics*, 77(1-2):41–47, 2014.

[7] C.-W. Shih. Complpete stability for a class of cellular neural networks. *International Journal of Bifurcation and Chaos*, 11(01):169–177, 2001.

[8] L. O. Chua and T. Roska. Stability of a class of nonreciprocal cellular neural networks. *IEEE Transactions on Circuits and Systems*, 37(12):1520–1527, 1990.

[9] S. Mohamad and K. Gopalsamy. Exponential stability of continuous-time and discrete-time cellular neural networks with delays. *Applied Mathematics and Computation*, 135(1):17–38, 2003.

[10] C. Huang, R. Su, J. Cao, and S. Xiao. Asymptotically stable high-order neutral cellular neural networks with proportional delays and D operators. *Mathematics and Computers in Simulation*, 171:127–135, 2020.

[11] C. Xu, M. Liao, P. Li, Z. Liu, and S. Yuan. New results on pseudo almost periodic solutions of quaternion-valued fuzzy cellular neural networks with delays. *Fuzzy Sets and Systems*, 411:25–47, 2021.

[12] M. Otkel, G. Soundararajan, R. Rakkiyappan, and A. Kashkynbayev. Finite-time/fixed-time synchronization of memristive shunting inhibitory cellular neural networks via sliding mode control. *Mathematics and Computers in Simulation*, 2023.

[13] I. Vida, M. Bartos, and P. Jonas. Shunting inhibition improves robustness of gamma oscillations in hippocampal interneuron networks by homogenizing firing rates. *Neuron*, 49(1):107–117, 2006.

[14] F. S. Chance and S. G. Cardwell. Shunting inhibition as a neural-inspired mechanism for multiplication in neuromorphic architectures. 2023.

[15] A. Bouzerdoum and R. B. Pinter. Shunting inhibitory cellular neural networks: derivation and stability analysis. *IEEE Transactions on Circuits and Systems I: Fundamental Theory and Applications*, 40(3):215–221, 1993.

[16] M. Akhmet, M. Tleubergenova, and A. Zhamanshin. Shunting Inhibitory Cellular Neural Networks with Compartmental Unpredictable Coefficients and Inputs. *Mathematics*, 11(6):1367–1367, 2023.

[17] J. Shao. Anti-periodic solutions for shunting inhibitory cellular neural networks with time-varying delays. *Physics Letters A*, 372(30):5011–5016, 2008.

[18] H. N. Cheung, A. Bouzerdoum, and W. Newland. Properties of Shunting Inhibitory Cellular Neural Networks for Colour Image Enhancement. 2003.

[19] X. Huang and J. Cao. Almost periodic solution of shunting inhibitory cellular neural networks with time-varying delay. *Physics Letters A*, 314(3):222–231, 2003.

[20] Y. Li, C.-C. Liu, and L. Zhu. Global exponential stability of periodic solution for shunting inhibitory CNNs with delays. *Physics Letters A*, 337(1-2):46–54, 2005.

[21] Q. Zhou, B. Xiao, Y. Yu, and L. Peng. Existence and exponential stability of almost periodic solutions for shunting inhibitory cellular neural networks with continuously distributed delays. *Chaos, Solitons* & *Fractals*, 34(3):860–866, 2007.

[22] L. Chen and H. Zhao. Global stability of almost periodic solution of shunting inhibitory cellular neural networks with variable coefficients. *Chaos, Solitons* & *Fractals*, 35(2):351–357, 2008.

[23] V. D. Milman and A. D. Myshkis. On the stability of motion in the presence of impulses. *Sibirskii Matematicheskii Zhurnal*, 1(2):233–237, 1960.

[24] Lakshmikantham Vangipuram, Bainov Drumi D, and S. Pavel. *Theory Of Impulsive Differential Equations*. World Scientific, 1989.

[25] Y. Wang and J. Lu. Some recent results of analysis and control for impulsive systems. *Communications in Nonlinear Science and Numerical Simulation*, 80:104862–104862, 2020.

[26] M.-J. Hu, J.-W. Xiao, R.-B. Xiao, and W.-H. Chen. Impulsive effects on the stability and stabilization of positive systems with delays. *Journal of the Franklin Institute*, 354(10):4034–4054, 2017.

[27] J. Lu, Daniel, and J. Cao. A unified synchronization criterion for impulsive dynamical networks. *Automatica*, 46(7):1215–1221, 2010.

[28] W. He, F. Qian, and J. Cao. Pinning-controlled synchronization of delayed neural networks with distributed-delay coupling via impulsive control. *Neural Networks*, 85:1–9, 2017.

[29] X. Li, D. Peng, and J. Cao. Lyapunov stability for impulsive systems via event-triggered impulsive control. *IEEE Transactions on Automatic Control*, 65(11):4908–4913, 2020.

[30] B. M. Miller and Evgeny Ya. Rubinovich. *Impulsive Control in Continuous and Discrete-Continuous Systems.* Springer Nature, 2003.

[31] Mouffak Benchohra. *Impulsive Differential Equations and Inclusions.* Hindawi Publishing Corporation, 2006.

[32] Marat Akhmet. *Principles of Discontinuous Dynamical Systems.* 2010.

[33] L. Shi, C. Zhang, and S. Zhong. Synchronization of singular complex networks with time-varying delay via pinning control and linear feedback control. *Chaos, Solitons & Fractals*, 145:110805, 2021.

[34] X. Lv, J. Cao, and L. Rutkowski. Dynamical and static multisynchronization analysis for coupled multistable memristive neural networks with hybrid control. *Neural Networks*, 143:515–524, 2021.

[35] T. Erneux. *Applied Delay Differential Equations.* Springer Nature, 2009.

[36] J. K. Hale and Sjoerd M. Verduyn Lunel. *Introduction to Functional Differential Equations.* 1993.

[37] I. Mezo. *The Lambert W Function.* CRC Press, 2022.

[38] Jerzy Zabczyk. *Mathematical Control Theory.* 2020.

[39] Zdzislaw Bubnicki. *Modern Control Theory.* Springer Science & Business Media, 2005.

[40] X. Yang and J. Cao. Finite-time stochastic synchronization of complex networks. *Applied Mathematical Modelling*, 34(11):3631–3641, 2010.

[41] S. P. Bhat and D. S. Bernstein. Finite-time stability of homogeneous systems. *Proceedings of the American Control Conference*, 1997.

[42] A. Kashkynbayev, A. Issakhanov, M. Otkel, and J. Kurths. Finite-time and fixed-time synchronization analysis of shunting inhibitory memristive neural networks with time-varying delays. *Chaos, Solitons & Fractals*, 156:111866, 2022.

[43] Y. Zhao, S. Ren, and J. Kurths. Finite-time and fixed-time synchronization for a class of memristor-based competitive neural networks with different time scales. *Chaos, Solitons & Fractals*, 148:111033–111033, 2021.

[44] C. Leondes, editor. *Techniques in Discrete and Continuous Robust Systems*. Academic Press, 1996.

[45] D. Zhang, Y. Shen, and J. Mei. Finite-time synchronization of multi-layer nonlinear coupled complex networks via intermittent feedback control. *Neurocomputing*, 225:129–138, 2017.

[46] S. Dong, X. Liu, S. Zhong, K. Shi, and H. Zhu. Practical synchronization of neural networks with delayed impulses and external disturbance via hybrid control. *Neural Networks*, 157:54–64, 2023.

[47] R. T. Stefani and E. Al. *Design of Feedback Control Systems*. Oxford University Press, 2002.

[48] X. Li, J. Fang, and H. Li. Finite-time synchronization and adaptive synchronization of memristive recurrent neural networks with delays. *International Journal of Adaptive Control and Signal Processing*, 2018.

[49] H.-L. Li, C. Hu, L. Zhang, H. Jiang, and J. Cao. Complete and finite-time synchronization of fractional-order fuzzy neural networks via nonlinear feedback control. *Fuzzy Sets and Systems*, 443:50–69, 2022.

[50] C. Hu, J. Yu, and H. Jiang. Finite-time synchronization of delayed neural networks with Cohen–Grossberg type based on delayed feedback control. *Neurocomputing*, 143:90–96, 2014.

[51] J. Mathew and F. Crevecoeur. Adaptive feedback control in human reaching adaptation to force fields. *Frontiers in Human Neuroscience*, 15, 2021.

[52] G. Tao, Santa Ram Joshi, and X. Ma. Adaptive state feedback and tracking control of systems with actuator failures. 46(1):78–95, 2001.

[53] T. Yang. *Impulsive Control Theory.* Springer-Verlag, 2001.

[54] J. Lu, D. W. C. Ho, J. Cao, and J. Kurths. Single impulsive controller for globally exponential synchronization of dynamical networks. *Nonlinear Analysis: Real World Applications*, 14(1):581–593, 2013.

[55] S. Dashkovskiy and P. Feketa. Input-to-state stability of impulsive systems and their networks. *Nonlinear Analysis: Hybrid Systems*, 26:190–200, 2017.

[56] S. Zhang, J. Sun, and Y. Zhang. Stability of impulsive stochastic differential equations in terms of two measures via perturbing Lyapunov functions. *Applied Mathematics and Computation*, 218(9):5181–5186, 2012.

[57] X. Lv and X. Li. Finite time stability and controller design for nonlinear impulsive sampled-data systems with applications. *ISA Transactions*, 70:30–36, 2017.

[58] Y. Liu and Donal O'Regan. Multiplicity results using bifurcation techniques for a class of boundary value problems of impulsive differential equations. *Communications in Nonlinear Science and Numerical Simulation*, 16(4):1769–1775, 2011.

[59] Z.-H. Guan and N. Liu. Generating chaos for discrete time-delayed systems via impulsive control. *Chaos: An Interdisciplinary Journal of Nonlinear Science*, 20(1), 2010.

[60] R. O. Grigoriev, M. C. Cross, and H. G. Schuster. Pinning control of spatiotemporal chaos. *Physical Review Letters*, 79(15):2795–2798, 1997.

[61] W. Yu, G. Chen, and J. Lü. On pinning synchronization of complex dynamical networks. *Automatica*, 45(2):429–435, 2009.

[62] X. F. Wang and G. Chen. Pinning control of scale-free dynamical networks. *Physica D: Nonlinear Phenomena*, 310(3-4):521–531, 2002.

[63] W. Yu, G. Chen, J. Lu, and J. Kurths. Synchronization via pinning control on general complex networks. *SIAM Journal on Control and Optimization*, 51(2):1395–1416, 2013.

[64] F. Chen, Z. Chen, L. Xiang, Z. Liu, and Z. Yuan. Reaching a consensus via pinning control. *Automatica*, 45(5):1215–1220, 2009.

[65] H. Liu, J. Li, Z. Li, Z. Zeng, and J. Lu. Intralayer synchronization of multiplex dynamical networks via pinning impulsive control. *IEEE Transactions on Cybernetics*, 52(4):2110–2122, 2022.

[66] X. Liu and T. Chen. Synchronization of Linearly Coupled Networks With Delays via Aperiodically Intermittent Pinning Control. 26(10):2396–2407, 2015.

[67] N. Mahdavi, M. B. Menhaj, J. Kurths, J. Lu, and A. Afshar. Pinning impulsive synchronization of complex dynamical networks. *International Journal of Bifurcation and Chaos*, 22(10):1250239, 2012.

[68] M. Akhmet, M. O. Fen, and M. Kirane. Almost periodic solutions of retarded SICNNs with functional response on piecewise constant argument. *Neural Computing and Applications*, 27(8):2483–2495, 2015.

[69] Y. Zou, X. Yang, R. Tang, and Z. Cheng. Finite-time quantized synchronization of coupled discontinuous competitive neural networks with proportional delay and impulsive effects. *Journal of the Franklin Institute*, 357(16):11136–11152, 2020.